

27. R. K. Dixon *et al.*, *Science* **263**, 185 (1994).
 28. I. A. Janssens *et al.*, *Science* **300**, 1538 (2003).
 29. J. Lloyd, G. D. Farquhar, *Funct. Ecol.* **10**, 4 (1996).
 30. S. R. Saleska *et al.*, *Science* **302**, 1554 (2003).
 31. K. W. Holmes *et al.*, *Global Biogeochem. Cycles* **20**, GB3004 (2006).
 32. A. D. McGuire *et al.*, *Global Biogeochem. Cycles* **15**, 183 (2001).
 33. D. F. Baker *et al.*, *Global Biogeochem. Cycles* **20**, GB1002 (2006).
 34. We thank the following T3L2 modelers for sharing their model output with us: R. M. Law, P. J. Rayner, D. Baker, Y.-H. Chen, I. Y. Fung, S. Houweling, J. John, T. Maki,

S. Maksyutov, P. Peylin, M. Prather, B. C. Pak, and S. Taguchi. We thank A. Jacobson for helpful discussions. This work was supported by funding from the NSF, which sponsors the National Center for Atmospheric Research. The Transcom 3 experiment was made possible through support from the NSF (OCE-9900310), the National Oceanic and Atmospheric Administration (NA67RJ0152, Amend 30), and the International Geosphere Biosphere Program/Global Analysis, Interpretation, and Modeling Project. The Zotino measurements are supported by the European Union through the TCOS-Siberia contract (EVK2-CT-2001-00131) within the Fifth Framework Program. The Bass Strait/Cape Grim aircraft sampling

program was supported by the Australian Bureau of Meteorology (1992–98), and the CSIRO Office of Space Science and Applications (1999–2000).

Supporting Online Material

www.sciencemag.org/cgi/content/full/316/5832/1732/DC1
 Materials and Methods
 SOM Text
 Figs. S1 to S9
 Tables S1 to S5
 References

31 October 2006; accepted 9 May 2007
 10.1126/science.1137004

Saturation of the Southern Ocean CO₂ Sink Due to Recent Climate Change

Corinne Le Quéré,^{1,2,3*} Christian Rödenbeck,¹ Erik T. Buitenhuis,^{1,2} Thomas J. Conway,⁴ Ray Langenfelds,⁵ Antony Gomez,⁶ Casper Labuschagne,⁷ Michel Ramonet,⁸ Takakiyo Nakazawa,⁹ Nicolas Metz,¹⁰ Nathan Gillett,¹¹ Martin Heimann¹

Based on observed atmospheric carbon dioxide (CO₂) concentration and an inverse method, we estimate that the Southern Ocean sink of CO₂ has weakened between 1981 and 2004 by 0.08 petagrams of carbon per year per decade relative to the trend expected from the large increase in atmospheric CO₂. We attribute this weakening to the observed increase in Southern Ocean winds resulting from human activities, which is projected to continue in the future. Consequences include a reduction of the efficiency of the Southern Ocean sink of CO₂ in the short term (about 25 years) and possibly a higher level of stabilization of atmospheric CO₂ on a multicentury time scale.

Atmospheric CO₂ increases at only half the rate of human-induced CO₂ emissions because of the presence of large CO₂ sinks in the ocean and on land (1). The sinks are highly variable and sensitive to climate, yet they are poorly constrained by observations. In the ocean, only the large-scale variability and trends in the equatorial and North Pacific have been quantified (2, 3). In other regions, time-series observations and repeated survey analysis exist, but their extrapolation at the scale of a basin is problematic because of the presence of large regional variability (4–6). Data are particularly sparse in the Southern Ocean, where the magnitude of the CO₂ sink is heavily disputed (7, 8), its interannual variability is unknown, and

its control on atmospheric CO₂ during glaciations is firmly established but still not understood or quantified (9, 10).

We estimated the variability and trend in the CO₂ sink of the Southern Ocean during 1981 to 2004 using the spatiotemporal evolution of atmospheric CO₂ from up to 11 stations in the Southern Ocean and 40 stations worldwide (Fig. 1). We used an inverse method that estimates the CO₂ flux distribution and time variability

that best matches the observed atmospheric CO₂ concentrations (11). The inversion uses observed atmospheric CO₂ concentrations from individual flask pair values and/or hourly values from in situ analyzers, as available (12) (fig. S1). The station set is kept constant throughout the inversion to minimize spurious variability from the inversion setup. We performed an identical inversion over four time periods using (i) 40 atmospheric stations for 1996 to 2004 (9 years), (ii) 25 atmospheric stations for 1991 to 2004 (14 years), (iii) 17 atmospheric stations for 1986 to 2004 time period (19 years), and (iv) 11 atmospheric stations for 1981 to 2004 (24 years). CO₂ fluxes and concentrations are linked by the atmospheric transport model TM3, with resolution of ~4° by 5° and 19 vertical levels, driven by interannual 6-hourly winds from National Centers for Environmental Prediction (NCEP) reanalysis (13). The a priori information does not involve any time-dependent elements. Although we focus on the Southern Ocean (south of 45°S), where the influence of the land is at its minimum, the inversion is global.

The variability in integrated sea-air CO₂ flux estimated by the inversions is ±0.14 Pg C year⁻¹ (14) over the Southern ocean (Fig. 2). The

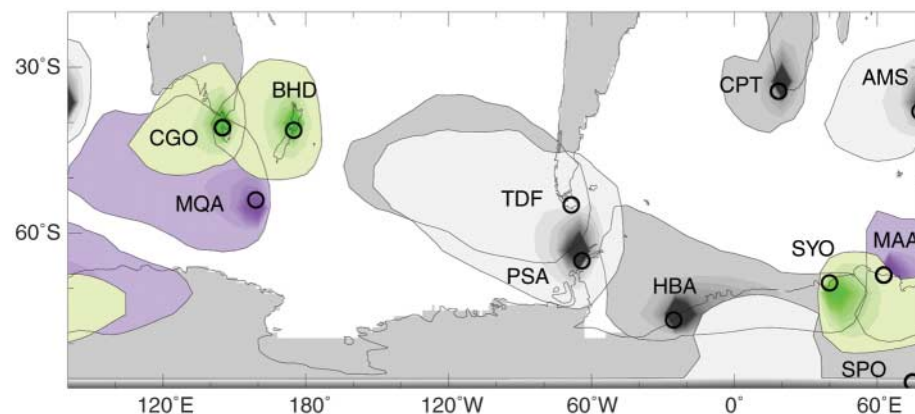


Fig. 1. Footprint of atmospheric CO₂ measurement stations. The footprint is defined here as the area where CO₂ fluxes of 0.2 mol/m² year⁻¹ produce a concentration response of at least 1 ppm, on an annual average. The darkest shading shows the region with largest influence on a given station. Stations are Cape Grim (CGO; 40.7°S, 144.7°E); Macquarie Island (MQA; 54°S, 159°E); Baring Head (BHD; 41°S, 175°E); Tierra del Fuego (TDF; 54.9°S, 68.5°W); Palmer Station (PSA; 65.0°S, 64°W); Halley Bay (HBA; 75.7°S, 25.5°W); Cape Point (CPT; 34°S, 19°E); Syowa (SYO; 69°S, 39°E); Mawson (MAA; 68°S, 63°E); Amsterdam Island (AMS; 38°S, 78°E); and South Pole (SPO; 90.0°S). The color coding refers to the length of the station's record used, with light gray stations used since 1981, green stations since 1986, purple stations since 1991, and dark gray stations since 1996.

¹Max Planck Institut für Biogeochemie, Postfach 100164, D-07701 Jena, Germany. ²School of Environmental Sciences University of East Anglia, Norwich NR4 7TJ, UK. ³British Antarctic Survey, High Cross, Madingley Road, Cambridge CB3 0ET, UK. ⁴National Oceanic and Atmospheric Administration, Earth System Research Laboratory, 325 Broadway, Boulder, CO 80305, USA. ⁵Commonwealth Scientific and Industrial Research Organisation, Marine and Atmospheric Research, PMB1 Aspendale, Victoria 3195, Australia. ⁶National Institute for Water and Atmospheric Research, P.O. Box 14901, Wellington, New Zealand. ⁷South African Weather Service, P.O. Box 320, Stellenbosch, 7599 South Africa. ⁸Laboratoire des Sciences du Climat et de l'Environnement/Institut Pierre Simon Laplace (LSCE/IPSL), Gif-sur-Yvettes, Cedex 91191, France. ⁹Center for Atmospheric and Oceanic Studies, Tohoku University, Sendai 980-8578, Japan. ¹⁰Laboratoire d'Océanographie et du Climat: Experimentation et Approches Numériques (LOCEAN/IPSL) CNRS, Université Pierre et Marie Curie, Paris, France. ¹¹Climate Research Unit, School of Environmental Sciences, University of East Anglia, Norwich NR4 7TJ, UK.

*To whom correspondence should be addressed. E-mail: c.lequere@uea.ac.uk

amplitude of the CO₂ variability is about one-third of the amplitude of the flux variability associated with El Niño events in the equatorial Pacific (2) and ~10% of the variability observed in atmospheric CO₂ growth rate (15). The longer inversion reproduces most of the variability of the shorter, better constrained inversions.

The longer inversion further shows a decrease of the CO₂ sink in the Southern Ocean between 1981 and 2004 by 0.031 Pg C year⁻¹ decade⁻¹. This decrease is significantly different at the 99.5% level (16) from the trend of -0.051 Pg C year⁻¹ decade⁻¹ in sea-air flux expected in response to the increase in atmospheric CO₂ alone (Fig. 2). We estimated the trend caused by increasing atmospheric CO₂ alone using two independent methods. First, we used a simple pulse response function, which we integrated in time using the observed atmospheric CO₂ growth rate as input (top red curve in Fig. 2) (12, 17). This method takes into account the surface ocean equilibration with atmospheric CO₂ and the vertical transport of anthropogenic carbon into the ocean. Second, we used a full Ocean General Circulation Model (OGCM) coupled to a state-of-the-art biogeochemistry model [the Pelagic Interactions Scheme for Carbon and Ecosystem Studies version T (PISCES-T) model; bottom red curve in Fig. 2] (12), which we forced with atmospheric surface conditions from either years 1948, 1967, or 1979 repeatedly for all years (three separate simulations, only the 1967 result is plotted in Fig. 2), and with observed atmospheric CO₂ concentration. The pulse response and OGCM estimates have similar variability and a similar trend over the 1981 to 2004 time period (-0.051 and -0.057; -0.046, and -0.072 Pg C year⁻¹ decade⁻¹, respectively) (Figs. 2 and 3).

The significant difference between the observed decrease of the CO₂ sink estimated by the inversion (0.03 Pg C year⁻¹ decade⁻¹) and the expected increase due solely to rising atmospheric CO₂ (-0.05 Pg C year⁻¹ decade⁻¹) indicates that there has been a relative weakening of the Southern Ocean CO₂ sink (0.08 Pg C year⁻¹ per decade⁻¹) as a result of changes in other atmospheric forcing (winds, surface air temperature, and water fluxes). For comparison, the mean Southern Ocean CO₂ sink is estimated to be between 0.1 and 0.6 Pg C year⁻¹ (table S1).

Inverse methods are sensitive to errors in the setup and transport model, in the data, and in the selection of the sites. We performed three series of sensitivity tests on the inversion results using the longest inversion. In the first series of tests, we assessed the robustness of the results to the choice of the most sensitive parameters of this inversion set up (11): (Is1 and Is2) We increased and decreased, respectively, the a priori standard deviation of the ocean and land CO₂ fluxes by a factor of four; (Is3) we increased the a priori standard deviation over the ocean and decreased that over land by a factor of 2 each; (Is4) we increased the spatial correlation scales by a factor

of 2 (in latitude) and 4 (in longitude); and (Is5) we decreased the temporal correlation scale by a factor of 4. In the second series of tests, we assessed the robustness of the results with respect to transport errors by degrading the quality of the transport model: (It1) we reduced the resolution of the transport model by a factor of two; and (It2

and It3) we used the degraded model It1 and applied constant winds for years 1990 and 1995, respectively. In the third series of tests, we used the degraded model It1 and included further available data from (Id1) Baring Head, (Id2) Halley Bay, and (Id3) Cape Grim and Syowa, even though they are not available over all the period.

Fig. 2. Sea-air CO₂ flux anomalies in the Southern Ocean (Pg C year⁻¹). The contribution of atmospheric CO₂ alone (top red curve) is calculated based on observed atmospheric CO₂ concentration and a pulse response function that computes the ocean CO₂ uptake as a function of time (12, 17). The estimates based on observations use an inverse model of atmospheric CO₂. Inversions over four time scales are shown starting in 1981 (thin black, 11 sites), 1986 (green, 17 sites), 1991 (purple, 25 sites), and 1996 (thick black, 40 sites). The gray shading encompasses results from all the sensitivity tests using the 11-site inversion. The lower panel shows results from a process model forced by (full red curve) the 1967 constant winds and fluxes and (blue curve) observed daily winds and fluxes from NCEP reanalysis. Sea-air CO₂ fluxes are integrated over 45°S to 90°S. Negative values indicate a flux of CO₂ from the atmosphere to the ocean, or a CO₂ sink into the ocean. Variability <1 year is removed using a Hanning filter for all time series. The 1995 to 2004 average was removed from all inversions (see table S1 for the spread in the mean). The mean of the atmospheric contribution is normalized to the inverted estimate for the 1981 to 1986 time period.

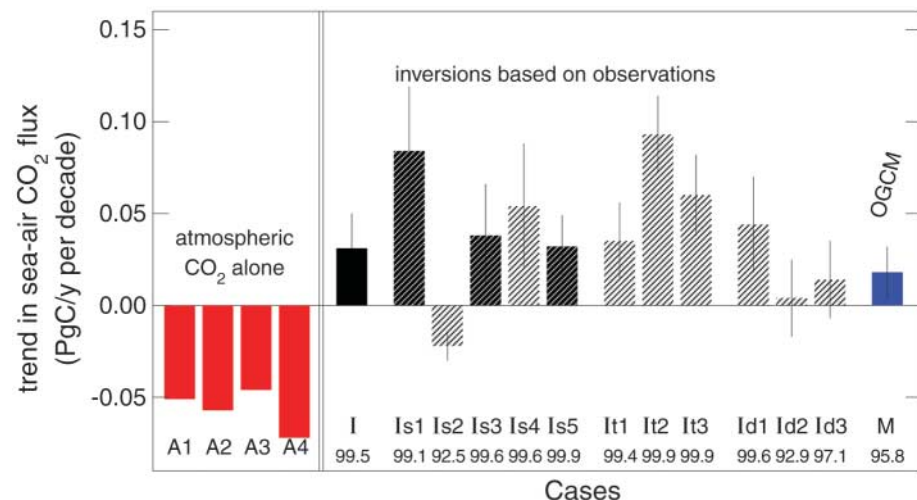
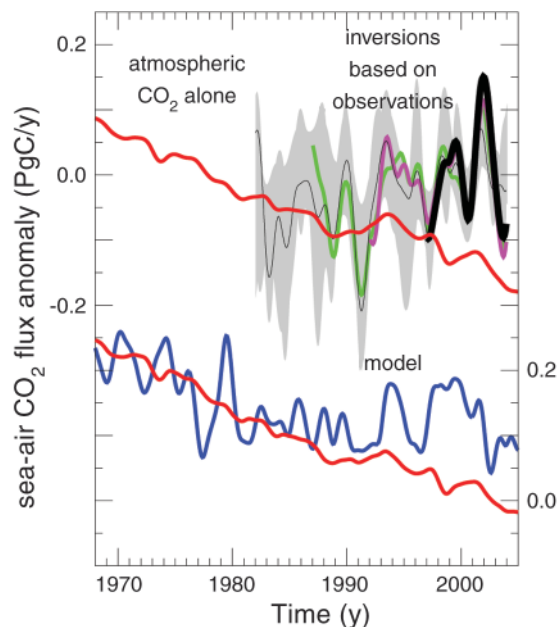


Fig. 3. Trend in the sea-air CO₂ flux (Pg C year⁻¹ decade⁻¹). Cases A1 to A4 estimate the contribution of atmospheric CO₂ alone based on a pulse response model (A1) and an OGCM forced by constant winds and atmospheric fluxes (A2 to A4) from years 1948, 1967, and 1979, respectively. All inverse results are shown in black or gray. Case I is the standard inversion. Cases Is1 to Is5 are sensitivity tests to the model parameters. Cases It1 to It3 are sensitivity tests to the atmospheric transport model. Cases Id1 to Id3 are sensitivity tests to the selection of data. The sensitivity tests hatched dark produce the best match to the station data, whereas those hatched light produce the poorest match (18). Results of the process model using observed atmospheric forcing are shown in blue (M). Error bars for all cases indicate the amplitude of the interannual variability (± 1 SD). Significance of the departure between all the inversion cases and case A1 and between the model M and case A3 is also shown below each case (16).

In all the sensitivity tests, the trend in the CO₂ sink in the Southern Ocean is smaller than the trend caused by increasing atmospheric CO₂ alone (Fig. 3). Inversions I (standard inversion), Is1, Is3, and Is5 produced the best fit to observations (18). These inversions showed a decrease in CO₂ sink of 0.03 to 0.08 Pg C year⁻¹ decade⁻¹, significantly different at the 99% level from the trend caused by atmospheric CO₂ alone (16). The inversions with the degraded transport model fit less well to the station data but still show a decrease in the CO₂ sink significantly different at the 99% level from the expected trend. The only sensitivity test that produces an increase in the CO₂ sink (Is2) also produces the worst fit to the observations (18). However, even this inversion produces a smaller increase in the CO₂ sink than that caused by atmospheric CO₂ alone, although the significance level is lower (92.5%).

We assessed the influence of the choice of stations further by comparing the trends in the long inversion with that of the 1986 to 2004 inversion, which uses 17 atmospheric stations instead of 11 (3 additional Southern Ocean stations). The trend in sea-air CO₂ flux in the two inversions for the overlapping period is similar, with 0.047 and 0.035 Pg C year⁻¹ decade⁻¹ for the 11-station and 17-station inversion, respectively, showing that the trend is correctly captured in the longer inversion.

The CO₂ flux variability from the longest inversion correlates with the Southern Annular Mode (SAM), an index of the dominant mode of atmospheric variability in the Southern Ocean. We use the SAM definition of Marshall (2003) (19), based on the difference in mean sea level pressure between 40°S and 65°S, which is entirely based on observations and fully independent of our inversion. The correlation of the monthly mean anomalies is small ($r = +0.22$) but significant at the 99% level (16, 18). The positive correlation indicates that the ocean outgasses CO₂ compared with its mean state when the SAM is positive, i.e., when the winds are intensified south of 45°S (20), and suggests that wind-driven upwelling and associated ventilation of the subsurface waters rich in carbon dominates the variability in CO₂ flux (18).

To examine whether the results of the inversion can be traced back to physical processes, we estimated the variability and trend in CO₂ fluxes using the OGCM-PISCES-T model (12), now forced by daily wind stress and heat and water fluxes from the NCEP reanalyzed data for 1948 to 2004 (13), similar to (21). This process model reproduces similar patterns of variability in CO₂ flux as estimated by the inversion, with a smaller CO₂ sink (more positive sea-air CO₂ flux) during 1993 to 2003 compared with 1983 to 1993 and 2003 to 2004 (Fig. 2). The process model also produces a decrease in the CO₂ sink between 1981 and 2004 of 0.018 Pg C year⁻¹ decade⁻¹ (Fig. 3). The difference in sea-air CO₂ trend of +0.064 Pg C year⁻¹ decade⁻¹ between this simulation using observed atmospheric forcing and the simulation using constant forcing (−0.046 Pg C year⁻¹

decade⁻¹ using 1967 forcing) is entirely attributable to changes in ocean biogeochemistry caused by changes in surface atmospheric forcing. Thus, the process model attributes the decrease in CO₂ sink to an increase in outgassing of natural carbon (sea-air flux of +0.064 Pg C year⁻¹ decade⁻¹) overcompensating the increase in the uptake of anthropogenic CO₂ (sea-air flux of −0.046 Pg C year⁻¹ decade⁻¹), in agreement with results of the inversion based on observations.

We performed two additional simulations. First, the winds alone were kept constant at year 1967, but the heat and water fluxes were allowed to vary interannually. Results from this simulation show a trend in sea-air CO₂ flux that is close to the simulation where both winds and fluxes are kept constant (−0.034 compared with −0.046 Pg C year⁻¹ decade⁻¹). Second, the winds were kept constant in the formulation of the gas exchange only but were allowed to vary in the physical model. The difference in trend with the variable gas exchange was very small (<3%). The results of the process model suggest that the changes in the CO₂ sink are dominated by the impact of changes in physical mixing and upwelling driven by changes in the winds on the natural carbon cycle in the ocean (18) (fig. S5), as suggested by the positive correlation between the inversion and the SAM. The process model also shows that the acidification of the surface ocean is accelerated by this process (18) (fig. S5).

On a multcentury time scale, results of simple models based on well-known carbon chemistry show that the ocean should take up 70 to 80% of all the anthropogenic CO₂ emitted to the atmosphere (22). This estimate takes into account changes in carbon chemistry but not the physical response of the natural carbon cycle to changes in atmospheric forcing. In the past, the marine carbon cycle has responded to circulation changes and cooling during glaciations by taking up enough carbon to lower atmospheric CO₂ by 80 to 100 parts per million (ppm) (9). Changes in Southern Ocean circulation resulting from changes in Southern Ocean winds (23) or buoyancy fluxes (24) have been identified as the dominant cause of atmospheric CO₂ changes (9, 10, 25). We showed that the Southern Ocean is responding to changes in winds over a much shorter time scale, thus suggesting that the long-term equilibration of atmospheric CO₂ in the future could occur at a level that is tens of ppm higher than that predicted when considering carbon chemistry alone.

Observations suggest that the trend in the Southern Ocean winds may be a consequence of the depletion of stratospheric ozone (26). Models suggest that part of the trend may also be caused by changes in surface temperature gradients resulting from global warming (27, 28). Climate models project a continued intensification in the Southern Ocean winds throughout the 21st century if atmospheric CO₂ continues to increase (28). The ocean CO₂ sink will persist as long as atmospheric CO₂ increases, but (i) the fraction of the CO₂ emissions that the ocean is able to absorb

may decrease if the observed intensification of the Southern Ocean winds continues in the future and (ii) the level at which atmospheric CO₂ will stabilize on a multcentury time scale may be higher if natural CO₂ is outgassed from the Southern Ocean.

References and Notes

1. I. C. Prentice *et al.*, in *Climate Change 2001: The Scientific Basis. Contribution of Working Group I to the Third Assessment Report of the Intergovernmental Panel on Climate Change*, J. T. Houghton, Y. Ding, D. Griggs, M. Noguer, P. van der Linden, X. Dai, K. Maskell, C. Johnson, Eds. (Cambridge Univ. Press, Cambridge and New York, 2001), pp. 183–237.
2. R. A. Feely, R. Wanninkhof, T. Takahashi, P. Tans, *Nature* **398**, 597 (1999).
3. T. Takahashi, S. C. Sutherland, R. A. Feely, R. Wanninkhof, *Deep-Sea Res.* **111**, 10.1029/2005JC002074 (2006).
4. N. Gruber, C. D. Keeling, N. R. Bates, *Nature* **298**, 2374 (2002).
5. J. E. Dore, R. Lukas, D. W. Sadler, D. M. Karl, *Nature* **424**, 754 (2003).
6. A. Corbière, N. Metzl, G. Reverdin, C. Brunet, T. Takahashi, *Tellus*, doi:10.1111/j.1600-0889.2006.00232.x (2007).
7. T. Roy, P. Rayner, R. Francey, *Tellus* **55B**, 701 (2003).
8. N. Metzl, C. Brunet, A. Jabaud-Jan, A. Poisson, B. Schauer, *Deep-Sea Res.* **53**, 1548, 10.1016/j.dsr.2006.07.006 (2006).
9. D. M. Sigman, E. Boyle, *Nature* **407**, 859 (2000).
10. K. E. Kohfeld, C. Le Quééré, S. P. Harrison, R. Anderson, *Science* **308**, 74 (2005).
11. C. Rödenbeck, Tech. Rep. 6, Max-Planck-Institute for Biogeochemistry, P.O. Box 100164, 07701 Jena, Germany, 2005. Available on www.bgc-jena.mpg.de/mpg/website/Biogeochemie/Publikationen/Technical_Reports/tech_report6.pdf.
12. See full description in Supporting Online Material, including a comparison to other published inversions (fig. S2).
13. E. Kalnay *et al.*, *Bull. Am. Meteorol. Soc.* **77**, 437 (1996).
14. 0.28 Pg C year⁻¹ for the peak-to-peak monthly anomalies in the longest inversion (1981 to 2004), equivalent to a standard deviation of 0.06 Pg C year⁻¹.
15. C. D. Keeling, T. P. Whorf, in *Trends: A Compendium of Data on Global Change* (Carbon Dioxide Information Analysis Center, Oak Ridge National Laboratory, U.S. Department of Energy, Oak Ridge, TN, 2005).
16. The statistical significance of the trend was estimated using the deseasonalized raw data and a 1000-member Monte Carlo ensemble from a noise model with the same standard deviation and lag-1 autocorrelation (12). The statistical significance only assesses the presence of a trend with respect to interannual variability and to random errors in the measurements. The significance of other errors and potential biases caused by the data coverage and inversion setup is assessed by the various sensitivity tests. The trend in the inversion result is not statistically different from zero, but from its expected value based on the increase in atmospheric CO₂ alone.
17. I. G. Enting, T. M. L. Wigley, M. Heimann, *CSIRO Aust. Div. Atmos. Res. Tech. Pap. No.* **31**, 1 (1994).
18. See further model results and evaluation in Supporting Online Material.
19. G. Marshall, *J. Clim.* **16**, 4134 (2003).
20. The increase in zonal winds is best documented by the observed increase in atmospheric pressure gradient between 40°S and 65°S (19). The NCEP reanalysis estimates an increase in zonal wind of ~1 to 2 m/s south of 45°S for a mean zonal wind of ~2 to 10 m/s.
21. P. Wetzel, A. Winguth, E. Maier-Reimer, *Global Biogeochem. Cycles* **19**, 10.1029/2004GB002339 (2005).
22. D. E. Archer, H. Khesghi, E. Maier-Reimer, *Geophys. Res. Lett.* **24**, 405 (1997).
23. R. J. Toggweiler, J. L. Russel, S. Carlson, *Paleoceanogr.* **21**, 10.1029/2005PA001154 (2006).
24. A. J. Watson, A. C. Naveira Garabato, *Tellus* **58B**, 73 (2006).
25. E. W. Wolff *et al.*, *Nature* **440**, 491 (2006).
26. D. W. J. Thompson, S. Solomon, *Science* **296**, 895 (2002).